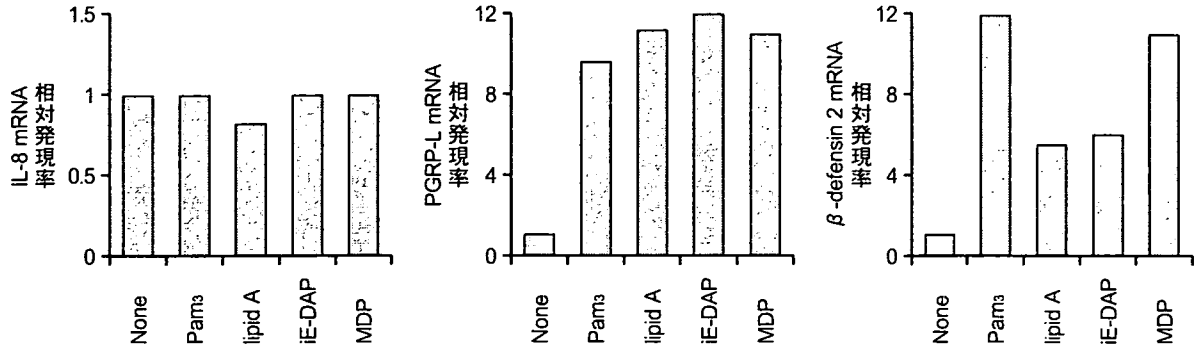

図3　NOD系およびTLR系刺激によるヒト上皮細胞からの抗菌ペプチド産生

口腔上皮系HSC-2細胞をTLR系（TLR2アゴニストの合成リポペプチドPam_3CSSNAとTLR4アゴニストの合成リピドA）およびNOD系（NOD1アゴニストのiE-DAPとNOD2リガンドのMDP）リガンドで刺激して，8時間目に細胞を回収し，全RNA抽出後RT-PCR法によりサイトカインならびに抗菌因子の遺伝子発現の動態を調べた。図にはIL-8，PGRP-Lおよびβ-defensin 2 mRNA発現の結果を示した。なお，結果はGAPDHの成績で補正して示している。

GAPDH：グリセルアルデヒド3-リン酸デヒドロゲナーゼ，IL：インターロイキン，MDP：ムラミルジペプチド，(m) RNA：(メッセンジャー) リボ核酸，PGRP：ペプチドグリカン認識タンパク，RT-PCR：逆転写ポリメラーゼ連鎖反応，TLR：Toll-like receptor　（文献18および未発表データに基づいて作成）

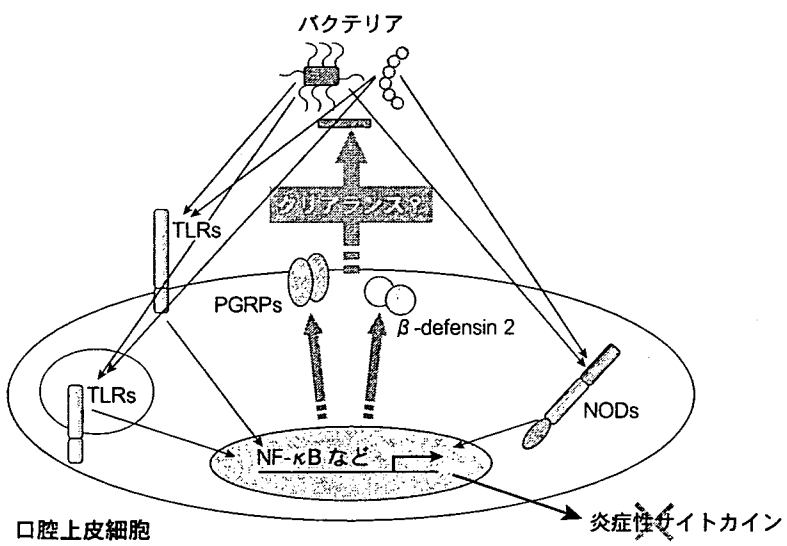

図4　上皮系細胞の細菌認識と自然免疫応答

上皮細胞での自然免疫応答は抗菌作用（β-defensin 2やPGRP等の産生）へと方向づけられており，炎症性応答は抑制されている。

NF-κB：nuclear factor-κB，PGRP：ペプチドグリカン認識タンパク，TLR：Toll-like receptor　（筆者ら作成）

ベルの炎症性サイトカインを産生する[19]。これらの知見を併せ考えると，細菌に常に接している口腔上皮細胞は，通常は細菌を認識しても炎症・免疫応答を発動しない状態に制御されているが，抗菌因子産生に関しては旺盛な応答性を有していると言えよう（図4）。

しかし，炎症状態に置かれた上皮細胞や細胞内に細菌の侵入を許した細胞は，菌体成分に応答してさらに強い炎症・免疫応答を惹起して，生体防御に当たろうとする。このような状況下で誘導される過剰な炎症・免疫応答が歯周組織破壊に結びつけば，歯周病発症の機転ともなり得る。

文　献

1) Akira S, Uematsu S, Takeuchi O : Pathogen recognition and innate immunity. Cell **124** : 783-801, 2006.
2) Fritz JH, Ferrero RL, Philpott DJ, et al : Nod-like proteins in immunity, inflammation and disease. Nat Immunol **7** : 1250-1257, 2006.
3) 浜田茂幸（編）：口腔微生物学・免疫学　第2版，医歯学出版，東京．p207-337，2005.
4) 小川知彦：*Bacteroides* 類縁菌 LPS の化学構造と免疫生物学的活性－ *Porphyromonas gingivalis* LPS 研究を中心に－．日細菌誌 **61** : 391-404，2006.
5) Asai Y, Ohyama Y, Gen K, et al : Bacterial fimbriae and their peptides activate human gingival epithelial cells through Toll-like receptor 2. Infect Immun **69** : 7387-7395, 2001.
6) Takada H, Kotani S : Immunopharmacological activities of synthetic muramyl-peptides. Immunology of the bacterial cell envelope (Stewart-Tull DES, Davies M ed). John Wiley & Sons, Chichester. p 119-152, 1985.
7) Takada H, Kotani S : Muramyl dipeptide and derivatives. The theory and practical application of adjuvants (Stewart-Tull DES ed). John Wiley & Sons. Chichester. p 171-202, 1995.
8) Adam A : Muramylpeptides and analogues. Synthetic adjuvants. John Wiley & Sons, New York. p1-58, 1985.
9) Goto T, and Aoki H : The immunomodulatory activities of acylpeptides. Immunostimulants : Now and tomorrow (Azuma I, Jollès G ed). Springer-Verlag. Berlin. p99-108, 1987.
10) Inohara N, Ogura Y, Fontalba A, et al : Host recognition of bacterial muramyl dipeptide mediated through NOD2. J Biol Chem **278** : 5509-5512, 2003.
11) Girardin SE, Boneca IG, Viala J, et al : Nod2 is a general sensor of peptidoglycan through muramyl dipeptide (MDP) detection. J Biol Chem **278** : 8869-8872, 2003.
12) Girardin SE, Boneca IG, Carneiro LAM, et al : Nod1 detects a unique muropeptide from Gram-negative bacterial peptidoglycan. Science **300** : 1584-1587, 2003.
13) Chamaillard M, Hashimoto M, Horie Y, et al : An essential role for NOD1 in host recognition of bacterial peptidoglycan containing diaminopimelic acid. Nat Immunol **4** : 702-707, 2003.
14) Uehara A, Fujimoto Y, Kawasaki A, et al : *Meso*-diaminopimelic acid and *meso*-lanthionine, amino acids specific to bacterial peptidoglycans, activate human epithelial cells through NOD1. J Immunol **177** : 1796-1804, 2006.
15) Barnard MR, Holt SC : Isolation and characterization of the peptidoglycans from selected Gram-positive and Gram-negative periodontal pathogens. Can J Microbiol **31** : 154-160, 1985.
16) Kato K, Umemoto T, Sagawa H, et al : Lanthionine as an essential constituent of cell wall peptidoglycan of *Fusobacterium nucleatum*. Curr Microbiol **3** : 147-151, 1979.
17) Sugawara Y, Uehara A, Fujimoto Y, et al : Toll-like receptors, NOD1, and NOD2 in oral epithelial cells. J Dent Res **85**:524-529, 2006.
18) Uehara A, Sugawara Y, Kurata S, et al : Chemically synthesized pathogen-associated molecular patterns increase the expression of peptidoglycan recognition proteins via Toll-like receptors, NOD1 and NOD2 in human oral epithelial cells. Cell Microbiol **7** : 675-686, 2005.
19) Uehara A, Sugawara S, Takada H : Priming of human oral epithelial cells by interferon-γ to secrete cytokines in response to lipopolysaccharides, lipoteichoic acids and peptidoglycans. J Med Microbiol **51** : 626-634, 2002.

話　題

cANCAによる単球・マクロファージ系細胞活性化*

上原亜希子**　高田春比古**

Key Words：cANCA, protease-activated receptor(PAR), NOD1/2, Toll-like receptors(TLRs), innate immunity

はじめに

好中球の産生するproteinase 3(PR3)に対する自己抗体cANCAはWegener肉芽腫症をはじめとするさまざまな炎症性疾患との関連が指摘されている[1)2)]．先にわれわれは，抗PR3抗体を，PR3を細胞表層に発現するヒト口腔上皮細胞に作用させると，protease-activated receptor(PAR)-2を介して細胞を活性化することを見出した[3)]．そこで，cANCAによるヒト単球・マクロファージ系細胞の自然免疫応答増幅の可能性を検討した．

Toll-like receptor(TLR)系分子およびNOD系分子を介する菌体表層成分の認識

自然免疫系は微生物に特徴的な構造(pathogen-associated molecular patterns；PAMPs)をパターン認識して宿主の生体防御を担っている．ヒトでは9種のTLR系分子が知られ，それぞれが特定のPAMPsを認識する[4)]．加えて，細菌細胞壁の骨格をなすペプチドグリカン(PGN)は，細胞内レセプターNOD1とNOD2分子によっても認識される[5)]．

PARを介する細胞活性化作用

PARファミリーは7回膜貫通型のG蛋白質共役型受容体の一つで，プロテアーゼによりtethered ligandの外側が切断されることにより，リガンドが受容体本体に結合しG蛋白を活性化する[6)]．PARファミリーにはこれまでにPAR-1からPAR-4までが報告されている．PAR-2は特に炎症との関連が指摘されており，アレルギー反応や浮腫形成などに深くかかわっている．たとえば，喘息の患者の気道上皮ではPAR-2の発現が顕著に亢進している[7)]．また，PAR-2を欠損させたマウスではアレルギー反応などの炎症性疾患が起こりにくい[8)]．これまでに，口腔上皮細胞[9)]や歯肉線維芽細胞[10)]もPARファミリーを介して炎症応答を営むことが報告されている．われわれはこれまでに，好中球酵素PR3はPAR-2を介して口腔上皮細胞を活性化すること[9)]，さらにPR3を細胞表層に発現するヒト口腔上皮細胞に抗PR3抗体を作用させると，PAR-2を介して同細胞を活性化すること[3)]を見出した(図1)．

Anti-neutrophil cytoplasmic antibody (ANCA)

ANCAは1982年にDaviesらによって慢性腎不全患者血清中に見出された[11)]．ANCAには2種類，cANCAとpANCAが知られており，cANCAはPR3に対する，pANCAはmyeloperoxidase(MPO)に対する自己抗体であるといわれている．Wegener肉芽腫症をはじめとして，ANCAとの関連性が指摘されている慢性炎症性疾患が次々と報告されている[1)2)12)13)]．口腔領域においても，慢性歯周病患者血清中のANCA抗体価は健常者に比べて上昇しているとの報告もある[14)15)]．

* The activation of monocytic cells by cANCA via TLRs and NODs.

** Akiko UEHARA, Ph.D., D.D.S. & Haruhiko TAKADA, Ph.D., D.D.S.: 東北大学大学院歯学研究科口腔微生物学分野〔〒980-8575 仙台市青葉区星陵町4-1〕; Department of Microbiology and Immunology, Tohoku University Graduate School of Dentistry, Sendai 980-8575, JAPAN

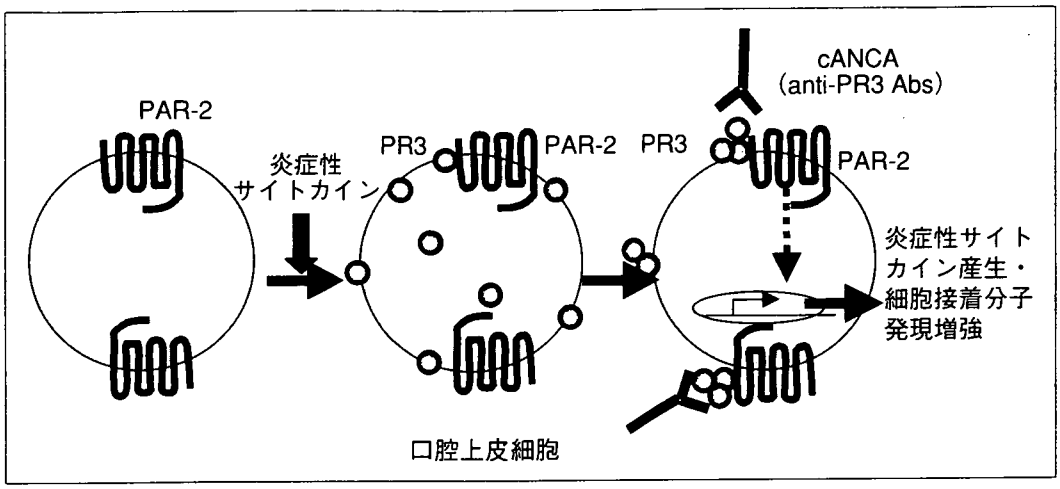

図1　cANCAによるPARを介する口腔上皮細胞活性化作用
口腔上皮細胞は恒常的にPAR-2を発現しているが，PR3は発現していない．炎症性サイトカインで処理すると口腔上皮細胞自身もPR3を発現する．同細胞を抗PR3抗体(cANCA)で刺激すると炎症性サイトカイン産生ならびに細胞接着分子発現が増強される．

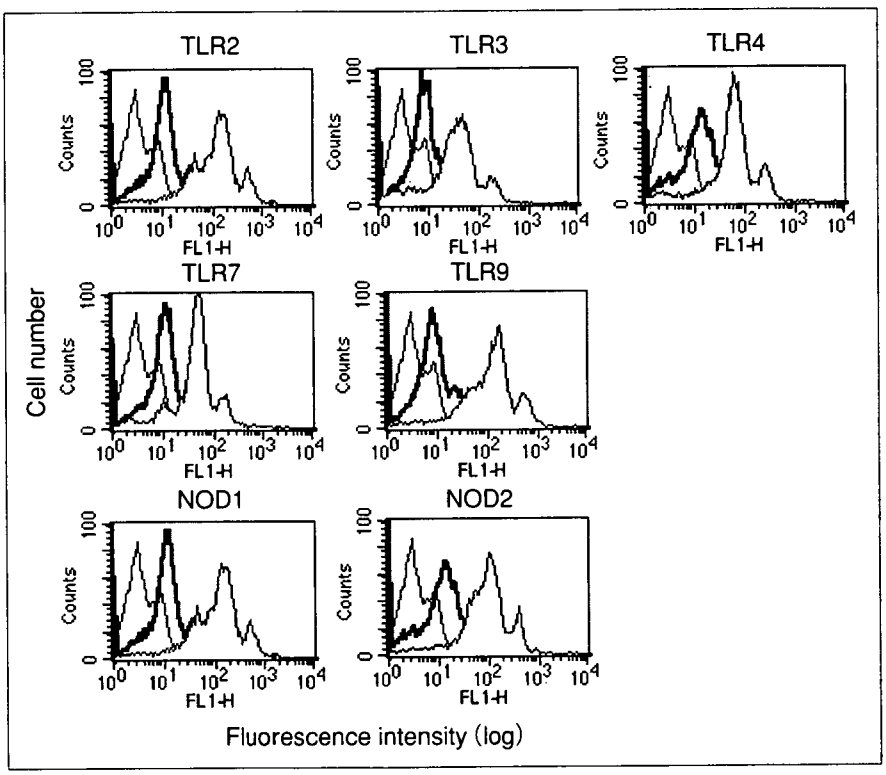

図2　抗PR3抗体刺激によりヒトPBMCsの各種TLR系ならびにNOD系分子発現が増強される
ヒトPBMCsを回収し，TLR2, 3, 4, 7, 9, NOD1および2分子を蛍光染色し，フローサイトメトリーによって解析した．抗PR3抗体処理細胞(灰色部分)，コントロール抗体処理細胞(太線)，横軸に蛍光強度(log)，縦軸に細胞数を示す．

cANCAによるPAR-2を介したヒト単球系細胞の自然免疫応答増幅作用

ヒト単球系THP-1およびヒト末梢血単核球(PBMCs)を抗PR3抗体あるいはコントロール抗体で24時間刺激後，フローサイトメトリーにより各種TLR系ならびにNOD系分子の発現を検討したところ，抗PR3抗体処理により同分子発現が顕著に増強された(図2)[16]．THP-1細胞およびPBMCsをWegener肉芽腫症患者から得たcANCA

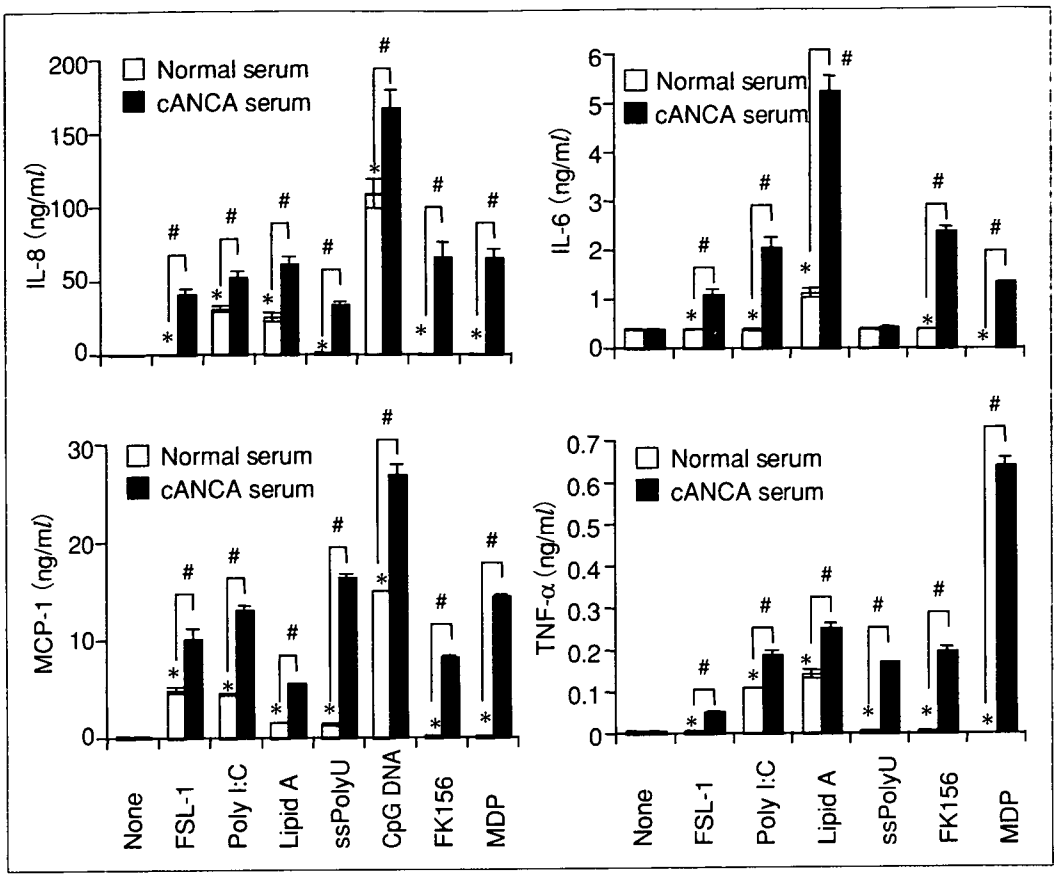

図3　cANCAでプライムされたヒトPBMCsをTLR系ならびにNOD系リガンドで刺激すると高レベルの炎症性サイトカインを産生する

PBMCsをコントロール血清(□)あるいはcANCA血清(■)処理後，各種TLR系ならびにNOD系リガンドで刺激して培養上清中のIL-8, IL-6, MCP-1およびTNF-α産生をELISA法により測定した．各種合成リガンド：1 nM FSL-1(TLR2/6リガンド)，10 μg/ml poly I:C(TLR3リガンド)，10 ng/ml lipid A(TLR4リガンド)，10 μg/ml ssPoly U(TLR7リガンド)，1 μM CpG DNA(TLR9リガンド)，100 μg/ml FK156(NOD1リガンド)，100 μg/ml MDP(NOD2リガンド)，*,# ANOVA検定により各対照群との間に有意差($P<0.01$)が認められた．

血清で24時間刺激後，各種TLR系ならびにNOD系リガンドで刺激して培養上清中の炎症性サイトカイン産生をELISA法により測定したところ，cANCA血清処理により各種TLR系ならびにNOD系リガンド刺激に高応答となり，高レベルの炎症性サイトカインを産生した(図3)[16]．cANCAによるプライミング作用のシグナル伝達系を調べるためにRNA干渉法によりPAR-2, PR3, NF-κBの遺伝子発現を特異的に抑制したトランスフェクタントを作成し，これらトランスフェクタントと親細胞を供試して比較検討したところ，cANCAによるヒト単球系細胞のプライミング作用はPAR-2, PR3, NF-κBを介して発揮されることが明らかとなった[16]．

おわりに

上記の研究成果に基づいて，われわれは「自己抗体cANCA存在下では，各種細胞の自然免疫応答が増幅されて，多臓器の肉芽腫形成を伴う慢性炎症性の自己免疫疾患を発症する」との作業仮説を立てた．すなわち，口腔ならびに副鼻腔の上皮細胞および血管内皮細胞では，cANCA刺激によってプライムされるとTLRないしNOD系刺激に応じて，高レベルの炎症性サイトカインを産生して，炎症状態が惹起される可能性がある．また，さまざまな組織においてcANCAでプライムされたマクロファージはTLRならびにNOD系刺激に高応答となり，過剰のサイトカインなどを産生し，さらにTLRとNOD系の相乗作用でさ

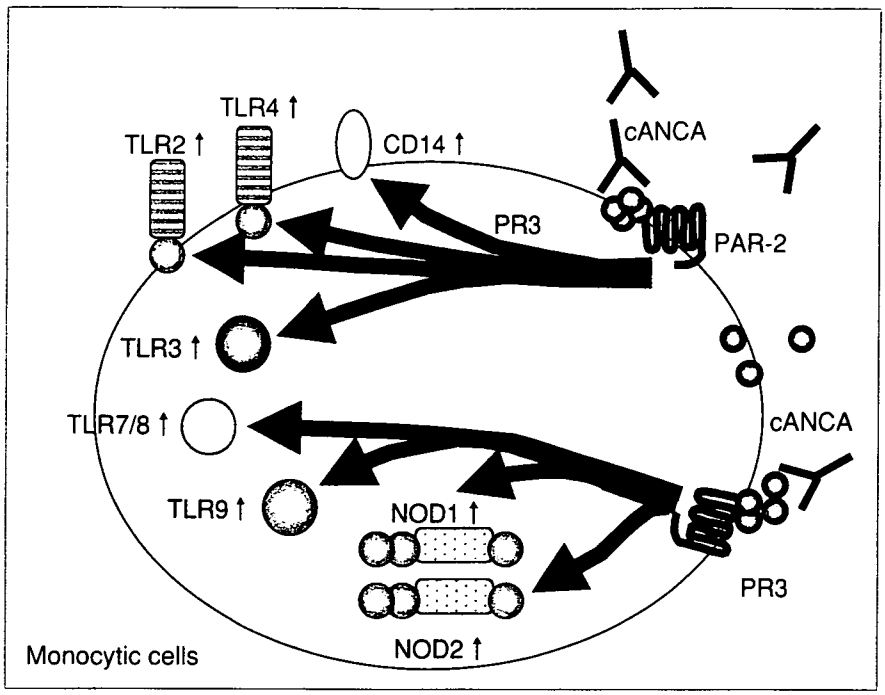

図4　ヒト単球・マクロファージ系細胞における自然免疫応答
cANCA存在下では単球・マクロファージ系細胞の自然免疫系レセプター発現が増強されて，対応するリガンド刺激に対する自然免疫応答が著しく亢進する．

らに反応が増幅される可能性がある(図4)．以上の可能性を実証できれば，Wegener肉芽腫症をはじめとするANCA関連自己免疫疾患の新たな病因論を提起できるのではないかと考えている．

文　献

1) Savige J, Davies D, Falk RJ, et al. Antineutrophil cytoplasmic antibodies and associated diseases : a review of the clinical and laboratory features. Kidney Int 2000 ; 57 : 846.
2) Bartůňková J, Tesař V, Šedivá A. Diagnostic and pathogenetic role of antineutrophil cytoplasmic autoantibodies. Clin Immunol 2003 ; 106 : 1.
3) Uehara A, Sugawara Y, Sasano T, et al. Proinflammatory cytokines induce proteinase 3 as membrane-bound and secretory forms in human oral epithelial cells and antibodies to proteinase 3 activate the cells through protease-activated receptor-2. J Immunol 2004 ; 173 : 4179.
4) Akira S, Uematsu S, Takeuchi O. Pathogen recognition and innate immunity. Cell 2006 ; 124 : 783.
5) Fritz JH, Ferrero RL, Philpott DJ, et al. Nod-like proteins in immunity, inflammation and disease. Nat Immunol 2006 ; 7 : 1250.
6) O'Brien PJ, Molino M, Kahn M, et al. Protease activated receptors : theme and variations. Oncogene 2001 ; 20 : 1570.
7) Knight DA, Lim S, Scaffidi AK, et al. Protease-activated receptors in human airways : up-regulation of PAR-2 in respiratory epithelium from patients with asthma. J Allergy Clin Immunol 2001 ; 108 : 797.
8) Lindner JR, Kahn ML, Coughlin SR, et al. Delayed onset of inflammation in protease-activated receptor-2-deficient mice. J Immunol 2000 ; 165 : 6504.
9) Uehara A, Sugawara S, Muramoto K, et al. Activation of human oral epithelial cells by neutrophil proteinase 3 through protease-activated receptor 2. J Immunol 2002 ; 169 : 4594.
10) Uehara A, Muramoto K, Takada H, et al. Neutrophil serine proteinases activate human nonepithelial cells to produce inflammatory cytokines through protease-activated receptor 2. J Immunol 2003 ; 170 : 5690.
11) Davies DJ, Moran JE, Niall JF, et al. Segmental necrotising glomerulonephritis with antineutrophil

antibody : possible arbovirus aetiology? Br Med J 1982 ; 285 : 606.

12) Hagen EC, Ballieux BE, van Es LA, et al. Antineutrophil cytoplasmic autoantibodies : a review of the antigens involved, the assays, and the clinical and possible pathogenetic consequences. Blood 1993 ; 81 : 1996.

13) Ardiles LG, Valderrama G, Moya P, et al. Incidence and studies on antigenic specificities of antineutrophil-cytoplasmic autoantibodies (ANCA) in poststreptococcal glomerulonephritis. Clin Nephrol 1997 ; 47 : 1.

14) Novo E, García-Mac Gregor E, Nava S, et al. A possible defective estimation of antineutrophil cytoplasmic antibodies in systemic lupus erythematosus due to the coexistence of periodontitis : preliminary observations. P R Health Sci J 1997 ; 16 : 369.

15) Novo E, Viera N. Antineutrophil cytoplasmic antibodies : a missing link in the pathogenesis of periodontal disease? J Periodontal Res 1996 ; 31 : 365.

16) Uehara A, Iwashiro A, Sato T, et al. Antibodies to proteinase 3 prime human monocytic cells via protease-activated receptor-2 and NF-κB for Toll-like receptor- and NOD-dependent activation. Mol Immunol 2007 ; 44 : 3552.

* * *

EXPERIMENTAL MEDICINE
実験医学 増刊

別　刷

羊土社
〒101-0052
東京都千代田区神田小川町2-5-1
TEL 03(5282)1211　FAX 03(5282)1212
E-mail：eigyo@yodosha.co.jp

口腔粘膜の自然免疫

上原 亜希子，菅原 由美子，高田 春比古

自然免疫系は昆虫からヒトに至る普遍的な機構であり，微生物に特有な分子構造（PAMP）をパターン認識して生体防御を担っている．PAMPを認識する受容体として，ヒトでは9種のTLR（Toll-like receptor）系分子と細胞内で細菌細胞壁ペプチドグリカン（PGN）などを認識するNOD系分子などが知られている．口腔粘膜の上皮細胞もTLR系ならびにNOD1/2分子を具備しているが，通常は炎症・免疫応答は抑制され，もっぱら抗菌因子産生にかかわっている．

はじめに

微生物に特有な構造PAMP（pathogen-associated molecular pattern）をパターン認識して生体防御を営む自然免疫系の解明が進んでいる．細胞膜上のTLR（Toll-like receptor）系分子は主として菌体成分を，細胞内エンドソームのTLR系分子は微生物に特徴的な核酸の配列を認識して侵襲微生物のセンサーとなっている[1]．さらに細胞内にはNOD系分子が存在し，細菌などの認識に携わっている[2]．

口腔には500～1,000種の細菌が生息するといわれている．これら細菌に恒常的に晒されている口腔上皮も，各種TLR系ならびにNOD系分子を発現している．しかし，正常な口腔上皮細胞を各種PAMPで刺激しても，炎症性サイトカインは誘導されない．本稿では，われわれが研究を進めている口腔粘膜組織の自然免疫系とその機能を中心に概説する．

1 TLR系分子を介する菌体成分の認識

自然免疫系は微生物に特徴的なPAMPをパターン認識してさまざまな反応を発動して宿主生体防御の基盤を担っている．審良静男ら（大阪大学・微生物病研究所）のノックアウトマウスを駆使した研究によって，10余種のTLR系分子が種々の細菌細胞表層成分や細

[キーワード&略語]
TLR, NOD1/2, PGN, 口腔上皮細胞, PGRP
ICAM：intercellular adhesion molecule
iE-DAP：γ-D-Glu-*meso*-DAP
IL：interleukin
meso-DAP：*meso*-diaminopimelic acid（メソジアミノピメリン酸）
PAMP：pathogen-associated molecular pattern
PGN：peptidoglycan（ペプチドグリカン）
PGRP：PGN recognition protein（ペプチドグリカン認識タンパク質）
TLR：Toll-like receptor（Toll様受容体）
TNF：tumor necrosis factor（腫瘍壊死因子）

Innate immunity in oral mucosa
Akiko Uehara[1]/Yumiko Sugawara[2]/Haruhiko Takada[1]：Department of Microbiology and Immunology, Tohoku University Graduate School of Dentistry/Division of Oral Diagnosis, Department of Oral Medicine and Surgery, Tohoku University Graduate School of Dentistry[2]（東北大学大学院歯学研究科口腔微生物学分野[1]/東北大学大学院歯学研究科口腔診断学分野[2]）

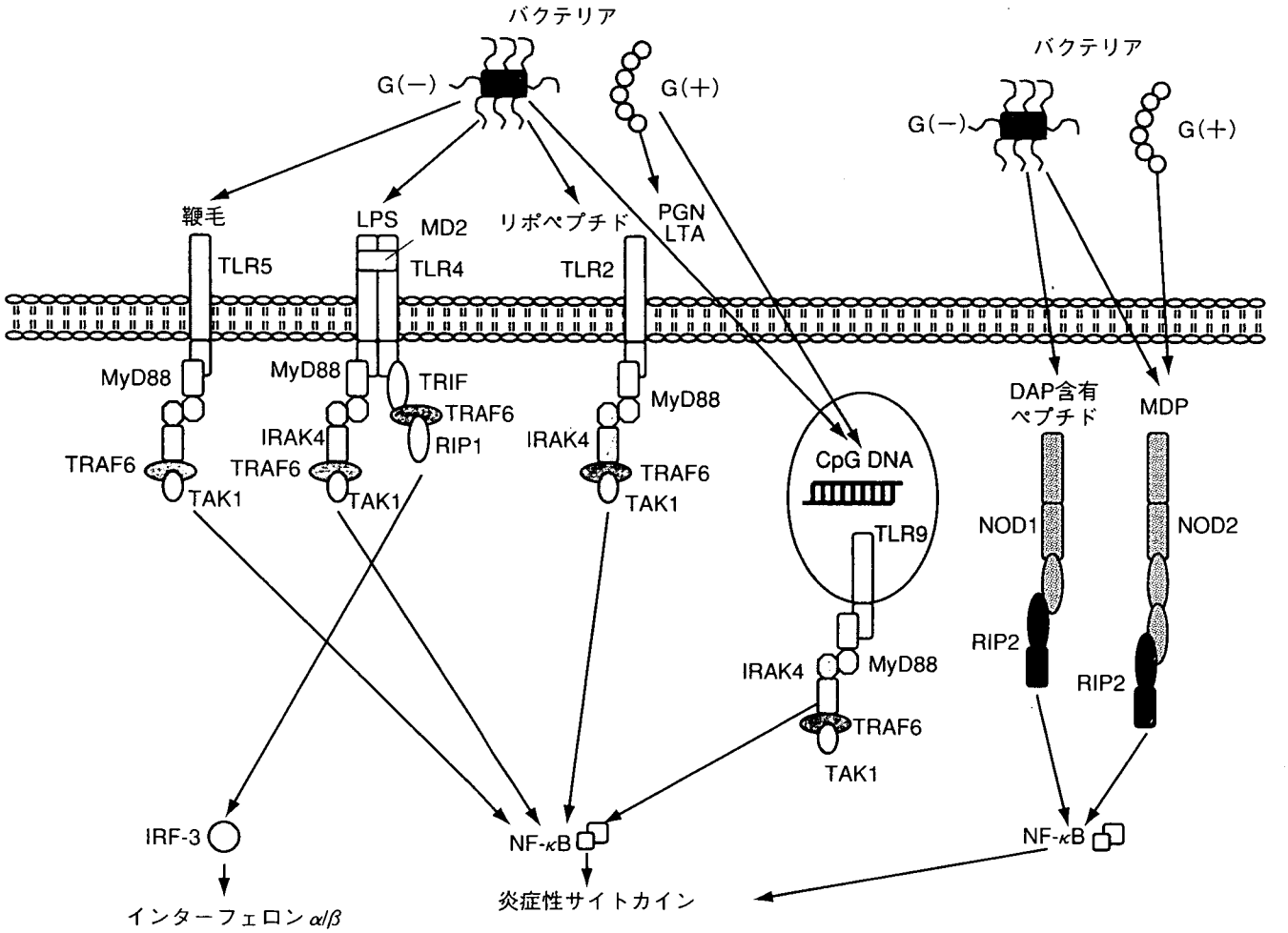

図1　TLR系およびNOD系を解するPAMPの認識機構
宿主細胞は侵襲微生物に共通して広く分布する菌体成分や特有の核酸配列（pathogen-associated molecular pattern：PAMP）をTLR系ならびにNOD系分子を介して認識し，自然免疫応答を示す（文献1より）

菌ならびにウイルスに特徴的な核酸配列を，それぞれ特異的に認識して宿主の生体防御を担うことが明らかにされた[1]．すなわち，マイコプラズマを除くほぼすべての細菌に存在するペプチドグリカン（peptidoglycan：PGN），細菌に普遍的なリポプロテイン，多くのグラム陽性菌に存在するリポタイコ酸（LTA）などは主としてTLR2によって，グラム陰性菌外膜成分の内毒素性リポ多糖（LSP）ないしリピドAはTLR4によって，細菌の運動器官である鞭毛はTLR5によって認識される．さらに細菌やウイルスに特徴的なDNAやRNA配列は，細胞内エンドソームに分布するTLR分子によって認識される．すなわちウイルスの二本鎖RNAはTLR3により，一本鎖RNAはTLR7/8により，細菌性CpG DNAはTLR9により認識される（図1）．

口腔細菌に関するこの方面のトピックスとして，歯周病原菌と目される*Porphyromonas gingivalis*をはじめとする*Bacteroides*類縁菌のリピドAは，大腸菌など腸内細菌科細菌のリピドAとは構造を異にしているため，生物活性がきわめて弱い．これは特異なリピドA構造のためにTLR4に認識されにくいためと考えられる．すなわち，これらの菌はグラム陰性菌センサーとしてのTLR4を回避して歯周組織に生息し続けるものと考えられる．ちなみに，*P. gingivalis*などの*Bacteroides*類縁菌のLPS（リピドA）はTLR2を活性化するとの多数の報告がある．しかし，小川知彦ら（朝日大学・歯学部）の研究によれば，これらTLR2活性は同菌LPS（リピドA）から通常の方法では分離できないリポペプチドに起因すると言う[3]．なお，*P. gingivalis*繊毛もTLR2に作用するといわれている[4]．ちなみにリポペプチドに関しては，柴田健一郎ら（北

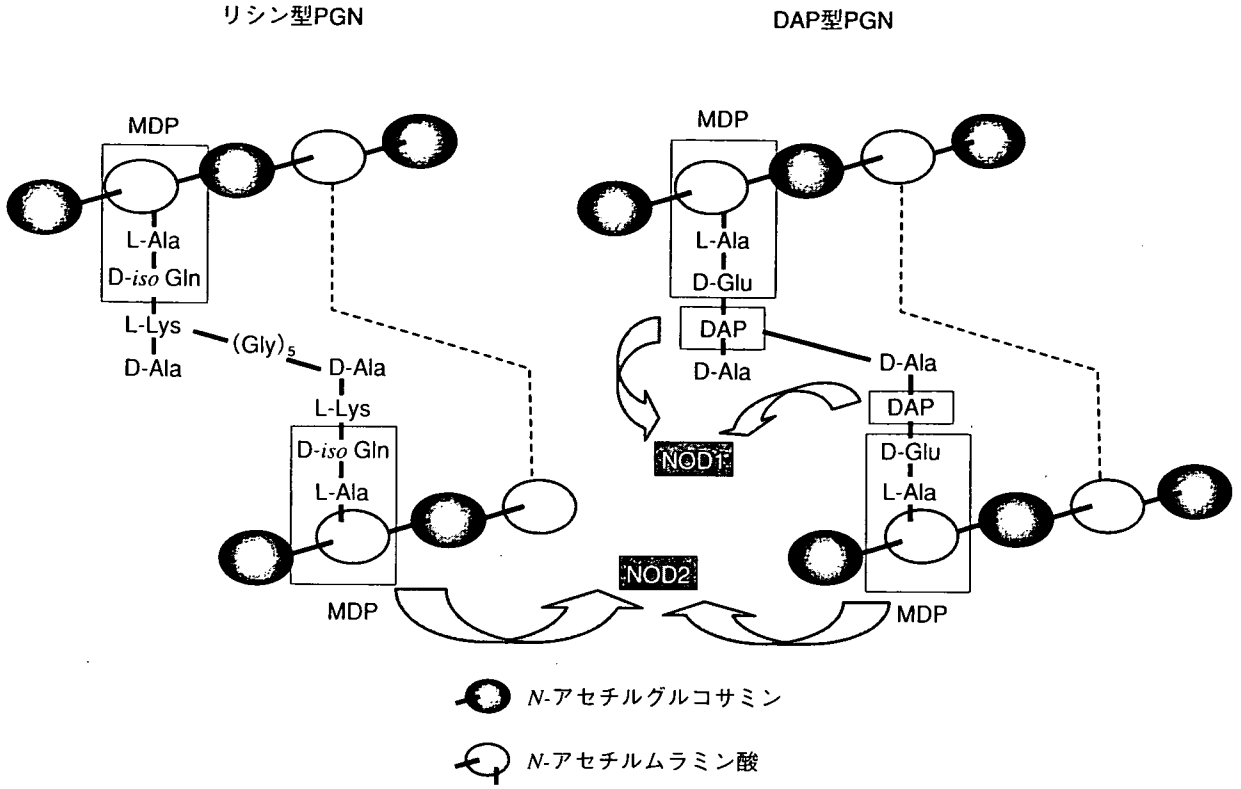

図2　PGNの構造とその活性部位
大部分のグラム陽性菌のPGNはリシン型，多くのグラム陰性菌と結核菌など一部のグラム陽性菌のPGNはDAP型である．PGNのMDP部分とDAP含有ペプチド部分を認識する細胞内受容体がNOD2とNOD1である

海道大学大学院・歯学研究科）が，マイコプラズマ型リポペプチドに始まり口腔細菌のそれを含めて広範な研究を進めている[5]．近年，TLR2活性化作用が歯周病に起因する心血管系の疾患に深くかかわるとの知見[6)~8)]とあわせ考えると興味深い．

2 NOD系分子を介する菌体成分の認識

PGNが示す多彩な生物活性の多くがムラミルジペプチド（Mur-NAc-L-Ala-D-isoGlu：MDP）によって担われていることから，MDPはアジュバント活性をはじめとするPGNの最小有効構造と目されてきた[9]．他方，PGNの別の活性構造としてジアミノピメリン酸（*meso*-diaminopimelic acid：*meso*-DAP）を含むペプチドフラグメントも化学合成され，MDPと同様の生物活性が報告されている[9]．前述したように，PGNはTLR2によって認識されるがその部分構造であるMDPはTLR2では認識されない[9]．2003年になって，MDPおよび*meso*-DAP含有ペプチドは，それぞれ細胞内受容体NOD2およびNOD1によって認識されることが証明された（図2）[10)~13)]．

3 口腔粘膜における自然免疫応答

1）口腔上皮細胞と歯肉線維芽細胞のTLR系ならびにNOD系分子発現

われわれの報告以前にも，口腔上皮細胞はTLR2を発現しているといわれていたが，TLR4発現に関しては否定的な報告が多かった．さらに，NOD系分子発現に関しては報告はなかった．われわれは口腔上皮細胞のプライマリーカルチャーならびに株化細胞と歯肉線維芽細胞を供試して，TLR系ならびにNOD系分子の遺伝子ならびにタンパク質発現を検討した．その結果，これらの細胞は恒常的にすべてのTLR系分子（TLR1～9），NOD1およびNOD2分子を明瞭に発現していることが明らかになった[14)~17)]．さらに，炎症歯肉組織は健常歯肉組織にくらべてTLR2およびTLR4発現が細胞辺縁に増強されることを組織学的に実証した（図3）[15)]．

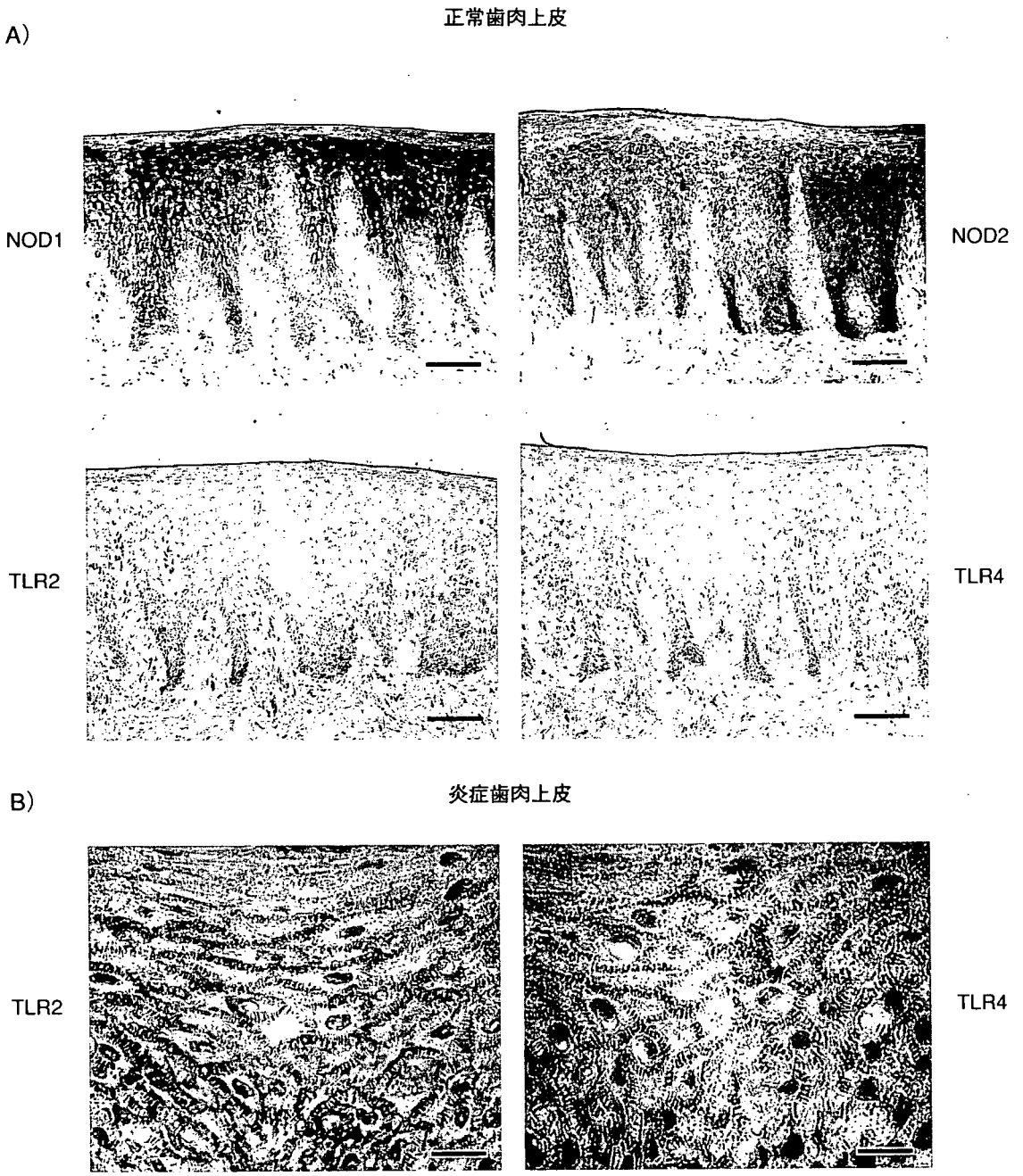

図3 歯肉組織のTLR系およびNOD系分子発現（巻頭カラー図3参照）
A）ヒト正常歯肉上皮にはNOD1ならびにNOD2分子が強く発現している（赤褐色）．またTLR2とTLR4も明確に発現している．B）炎症歯肉上皮ではTLR2とTLR4が細胞辺縁に局在する（AのBar：100 μm，BのBar：20 μm，文献15より転載）

2）上皮系細胞の自然免疫応答は炎症・免疫応答が抑制され，抗菌因子産生が活発である

口腔上皮細胞を各種化学合成リガンドで刺激した．供試した標品は，TLR2アゴニストの合成リポペプチドFSL-1，TLR3アゴニストのpoly I：C，TLR4アゴニストのリピドA，TLR7アゴニストのssPoly U，TLR9アゴニストのCpG DNA，NOD1アゴニストのiE-DAP（γ-D-Glu-*meso*-DAP）ならびにNOD2アゴニストのMDPである．その結果，いずれのリガンドで刺激しても，IL（interleukin）-8などの炎症性サイトカイン産生およびICAM（intercellular adhesion molecule）-1などの接着分子発現は増強されなかった[14) 15) 18)]．一方，これらのリガンド刺激によって，抗菌因子，すなわち4種のPGN認識タンパク質（PGN recognition

表1　各種上皮細胞のTLR系およびNOD系分子発現

ヒト上皮細胞	陽性細胞（%）					
	TLR2	TLR3	TLR4	TLR7	NOD1	NOD2
口腔上皮						
HSC-2	56.2	32.1	36.4	40.7	90.1	77.4
HO-1-u-1	48.9	38.8	33.0	41.6	85.4	70.8
咽頭上皮						
HEp-2	34.6	21.4	22.3	20.5	69.0	63.4
食道上皮						
TE-1	35.0	23.3	19.2	17.2	59.1	60.5
腸管上皮						
SW620	29.0	21.4	19.6	15.7	85.3	70.8
HT29	22.5	19.3	17.2	18.6	75.3	69.3
T84	11.4	8.9	9.2	12.2	48.2	44.7
Caco-2	9.6	8.1	7.7	9.4	39.8	33.8
子宮頚上皮						
HeLa	35.6	14.8	24.7	11.2	40.7	51.1

各種上皮細胞のTLR2, TLR3, TLR4, TLR7, NOD1およびNOD2発現をフローサイトメトリーにより解析した（文献16より）

protein：PGRP-L, -I α, -I βおよび-S）やベータディフェンシン2の産生が明瞭に増強された[14)~16) 19)]．ちなみに，炎症歯肉上皮組織ではこれら抗菌因子の発現が増強されていた（未発表）．さらに，口腔以外のさまざまなヒト上皮細胞（舌・唾液腺・咽頭・気道・腸管・肺・腎・肝・子宮頚）でもTLR2, 3, 4, 7, NOD1およびNOD2を恒常的に発現していることを証明した[16)]（表1）．これらの細胞を，各種TLR系およびNOD系リガンドで刺激すると，口腔上皮細胞と同様に，抗菌因子産生は活発に行うが，炎症性サイトカイン産生は抑制されているとの知見を得た[16)]．すなわち，口腔上皮細胞で得られた成績は，広く上皮細胞一般にも当てはまる現象と言える．

3）上皮細胞の炎症・免疫応答抑制の解除

口腔上皮細胞をインターフェロンガンマ，IL-1α，TNF（tumor necrosis factor）-αなどの炎症性サイトカインで前処理すると，上記TLR系ならびにNOD系リガンド刺激に応じて，高レベルの炎症性サイトカインを産生するようになる[20)]（および未発表データ）．これらの知見は，病的な条件下にある上皮細胞にあっては，炎症・免疫応答抑制機構が解除されることを示唆している．これと関連する知見として，歯周病原性細菌に特有な菌体成分で口腔上皮細胞を刺激した場合，明確な炎症性サイトカイン産生増強が認められた[21)]．

4）口腔粘膜の非上皮系細胞はTLR系およびNOD系リガンド刺激に応じて炎症性サイトカインを産生する

歯肉線維芽細胞はTLR系およびNOD系分子を恒常的に発現しており，対応するリガンド刺激に応答して炎症性サイトカインを産生した[17)]．さらに，炎症病巣で口腔粘膜に浸潤してくるヒト単球系細胞の応答を探る目的で，株化細胞THP-1を供試して実験を進めた．その結果，THP-1細胞をTLR系とNOD系リガンドを組合わせて同時に刺激すると相乗的な炎症性サイトカイン産生が認められることを明らかにした（図4）[22)]．

5）NOD1リガンドの再検討

これまでNOD1の最小有効リガンド構造はiE-DAPとされてきた．われわれは市販（シグマ社製）のDAPが単独で口腔上皮細胞を刺激してPGRP発現を増強するとの知見を得た．そこで深瀬浩一教授ら（大阪大学理学研究科）の協力を得て，化学合成した光学異性体（*meso*-DAP, LL-DAPおよびDD-DAP）を供試する実験を行った．その結果，*meso*-DAPあるいはメソランチオニン（*meso*-lanthionine）が単独でも各種ヒト上皮細胞のNOD1を活性化することを証明した[19)]．なお，LL-DAPは微弱な活性を示したが，DD-DAPは全く活性を欠いていた．ちなみに，グラム陰性菌の多く

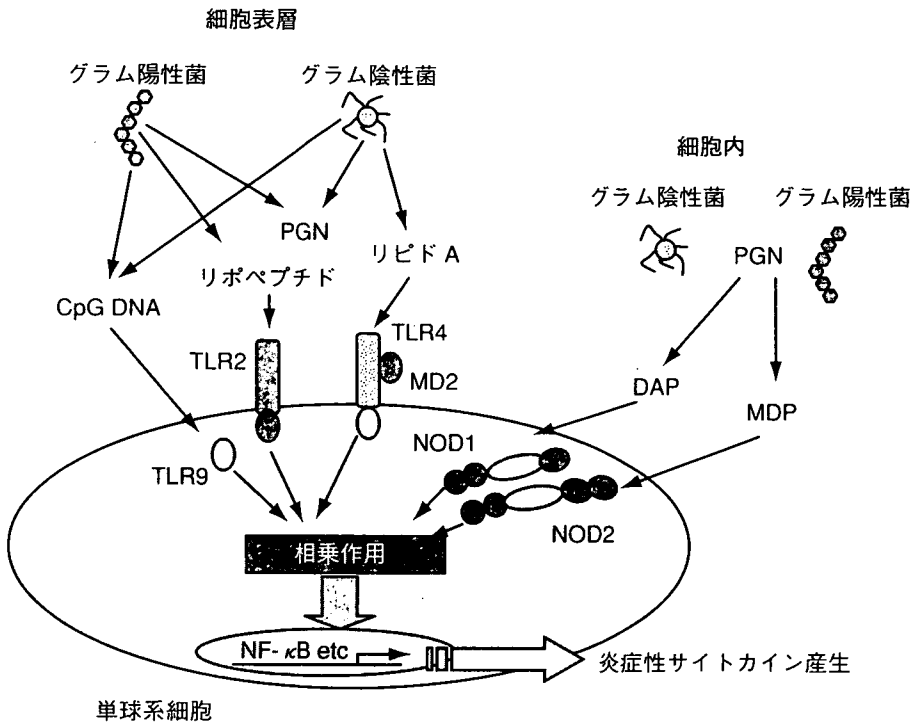

図4　単球系細胞の細菌に対する自然免疫
単球系細胞では細胞内のNOD1とNOD2分子を介して侵襲細菌を認識するその際，同時にTLRを介する細菌認識が起こるものと考えられる．NOD系とTLR系を介する刺激は宿主細胞の自然免疫応答を相乗的に誘導する

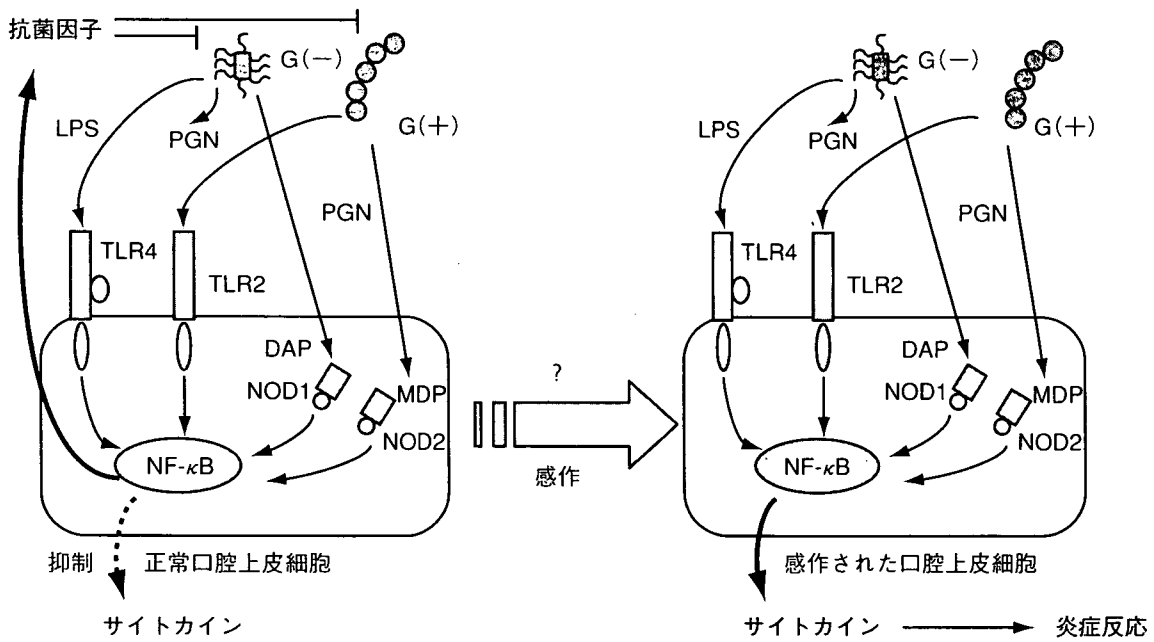

図5　口腔上皮細胞の細菌に対する自然免疫
正常口腔上皮細胞は菌体成分刺激に応じて抗菌因子を産生して感染を阻止する．他方，炎症部位の上皮細胞や感染上皮細胞はサイトカインを産生して炎症・免疫応答を導く

は *meso*-DAP型PGNを有するが，*P. gingivalis*のPGNはLL-DAP[23]を，しばしば口腔より分離される *Fusobacterium nucleatum*のPGNはメソランチオニン[24]を有している．なお，DD-DAPを有する細菌の報告はない．さらにLipofectamineやサイトカラシンDなどで細胞の膜透過性を高めた条件下では，単球系細胞でも *meso*-DAPはNOD1を活性化することを証明した[19]．

おわりに

ヒト口腔上皮細胞はTLR系やNOD系刺激を加えてもほとんどサイトカイン応答を示さないが，炎症性サイトカインでプライムされた細胞では同じ刺激に応じて高レベルの炎症性サイトカインを産生する．これらの知見は，細菌に常に接している口腔上皮細胞は，細菌を認識しても炎症・免疫応答を発動しない状態に制御されているが，抗菌因子産生に関しては旺盛な応答性を有していると言える．一旦炎症状態におかれた上皮細胞や細胞内に細菌の侵入を許した細胞は菌体成分に応答してさらに強い炎症・免疫応答を惹起して生体防御に当たるものと考えられる（図5）．他方，上皮細胞バリアが崩されて通常は微生物から隔離されていた非上皮系細胞が微生物に接すると，活発に炎症・免疫応答を示す．これらの反応があいまって歯周病に代表される炎症性組織破壊を齎すと考えられる．

文献

1）Akira, S. et al.：Cell, 124：783-801, 2006
2）Fritz, J. H. et al.：Nat. Immunol., 7：1250-1257, 2006
3）小川知彦：日細菌誌, 61：391-404, 2006
4）Asai, Y. et al.：Infect. Immun., 69：7387-7395, 2001
5）柴田健一郎：日細菌誌, 62：363-374, 2007
6）Hajishengallis, G. et al.：Ann. Periodontol., 7：72-78, 2002
7）Erridge, C. et al.：Cardiovasc. Res., 73：181-189
8）Triantafilou, M. et al.：Cell Microbiol., 9：2030-2039
9）Takada, H. & Uehara, A.：Curr. Pharm. Des., 12：4162-4172, 2006
10）Girardin, S. E. et al.：J. Biol. Chem., 278：8869-8872, 2003
11）Inohara, N. et al.：J. Biol. Chem., 278：5509-5512, 2003
12）Girardin, S. E. et al.：Science, 300：1584-1587, 2003
13）Chamaillard, M. et al.：Nat. Immunol., 4：702-707, 2003
14）Uehara, A. et al.：Cell Microbiol., 7：675-686, 2005
15）Sugawara, Y. et al.：J. Dent. Res., 85：524-529, 2006
16）Uehara, A. et al.：Mol. Microbiol., 44：3100-3111, 2007
17）Uehara, A. & Takada, H.：J. Dent. Res., 86：249-254, 2007
18）Uehara, A. et al.：Med. Microbiol. Immunol., 189：185-192, 2001
19）Uehara, A. et al.：J. Immunol., 177：1796-1804, 2006
20）Uehara, A. et al.：J. Med. Microbiol., 51：626-634, 2002
21）Sugiyama, A. et al.：J. Med. Microbiol., 51：27-33, 2002
22）Uehara, A. et al.：Cell Microbiol., 7：53-61, 2005
23）Barnard, M. R. & Holt, S. C.：Can. J. Microbiol., 31：154-160, 1985
24）Kato, K. et al.：Curr. Microbiol., 3：147-151, 1979

<筆頭著者プロフィール>

上原 亜希子：2003年東北大学大学院歯学研究科修了後，日本学術振興会特別研究員を経て，東北大学大学院歯学研究科助手．主に口腔上皮細胞の自然免疫系の解明を目指して研究を続けている．当研究室では大学院生募集中ですので，興味のある方はメール下さい．

E-mail：kyoro@mail.tains.tohoku.ac.jp

FEBS Letters 581 (2007) 3223–3229

Distinct roles of TIR and non-TIR regions in the subcellular localization and signaling properties of MyD88

Tadashi Nishiya*, Emi Kajita, Takahiro Horinouchi, Arata Nishimoto, Soichi Miwa

Department of Cellular Pharmacology, Hokkaido University Graduate School of Medicine, Sapporo 060-8638, Japan

Received 19 May 2007; accepted 6 June 2007

Available online 15 June 2007

Edited by Masayuki Miyasaka

Abstract MyD88 is a cytoplasmic adaptor protein that is critical for Toll-like receptor (TLR) signaling. The subcellular localization of MyD88 is characterized as large condensed forms in the cytoplasm. The mechanism and significance of this localization with respect to the signaling function, however, are currently unknown. Here, we demonstrate that MyD88 localization depends on the entire non-TIR region and that the correct cellular targeting of MyD88 is indispensable for its signaling function. The Toll-interleukin I receptor-resistance (TIR) domain does not determine the subcellular localization, but it mediates interaction with specific TLRs. These findings reveal distinct roles for the TIR and non-TIR regions in the subcellular localization and signaling properties of MyD88.

Keywords: MyD88; Non-TIR region; Signal transduction; Subcellular localization; TIR domain; TLR

1. Introduction

Toll-like receptors (TLRs) are key regulators in host defense mechanisms against infectious microorganisms [1]. More than 10 TLRs have been identified in mammals, all of which recognize highly conserved molecular structures in pathogens, ranging from bacterial cell-surface components to viral genomes. Ligand binding to a TLR initiates the recruitment of the Toll-interleukin I receptor-resistance (TIR) domain-containing adaptor proteins (TIR adaptors) to the cytoplasmic TIR domain of an activated TLR. TIR adaptors then initiate signaling events, eventually leading to the activation of the NF-κB, AP-1, and interferon regulatory factor (IRF) families of transcription factors, which induce the expression of genes involved in host defense against infection [2].

Four different TIR adaptors have been identified in mammals: MyD88, TIRAP/Mal, TRIF/TICAM1, and TRAM/TICAM2 [2]. MyD88 and TRIF play an essential role in downstream signaling, whereas TIRAP and TRAM may act to bridge the interaction of MyD88 and TRIF with specific TLRs. MyD88 is the first identified TIR adaptor that is essential for most TLR, IL-1 receptor, and IL-18 receptor signaling [3–7]. MyD88 is a protein of 296 amino acids and is composed of an N-terminal short region (N), a death domain (DD), an intermediate region (INT), and a C-terminal TIR domain. Previous research indicates that the TIR domain interacts with TLRs, whereas the DD is involved in downstream signaling. Several groups have reported the distinct subcellular localization of MyD88, which is characterized by condensed particles scattered throughout the cytosol [8–11]. Previous studies using CFP-YFP FRET analysis report a physical interaction between MyD88 and IRF-7 in these condensed particles [9,12]. Therefore, this distinct localization may be important for the signaling function of MyD88. However, the mechanism by which this localization is achieved is unknown, and its significance with respect to the function and structural features of MyD88 have not been studied in depth.

Each TIR adaptor interacts with specific TLRs and TIR adaptors. For example, MyD88 associates with all TLRs except TLR3, whereas TRIF only associates with TLR3 and TLR4. Furthermore, MyD88 and TRIF specifically interact with TIRAP and TRAM, respectively. There may be two factors that determine the specific partners for MyD88: a mechanical factor (e.g., specific TIR–TIR domain interaction) or a spatiotemporal factor (e.g., the distinct subcellular distributions of TLRs and TIR adaptors). However, the mechanism underlying the specificity of TLR–TIR adaptor and TIR adaptor–TIR adaptor interaction remains poorly understood.

Here, we report distinct roles for TIR and non-TIR regions with respect to the intracellular targeting of MyD88 and the interaction of MyD88 with specific TLRs and TIR adaptors. We found that the entire non-TIR region is responsible for the distinct subcellular localization of MyD88, and the correct cellular targeting of MyD88 is critical to its signaling function. In contrast, the TIR domain plays an essential role in determining the specificity of the MyD88–TLR interaction, whereas the specificity of the MyD88–TIRAP interaction was independent of the conformation of the TIR domain. These results not only describe the distinct roles of TIR and non-TIR regions in the subcellular localization and signaling properties of MyD88, they also provide evidence that the diversity of TLR signaling may be achieved by both TIR domain-dependent and -independent mechanisms.

*Corresponding author. Fax: +81 11 706 7824.
E-mail address: nishiya@med.hokudai.ac.jp (T. Nishiya).

Abbreviations: CFP, cyan fluorescent protein; CTXb, cholera toxin subunit b; DD, death domain; TIR, Toll-interleukin I receptor-resistance; TLR, Toll-like receptor; YFP, yellow fluorescent protein; INT, Intermediate region

0014-5793/S32.00
doi:10.1016/j.febslet.2007.06.008

2. Materials and methods

2.1. Reagents and cell cultures

Flagellin and CpG-B oligodeoxynucleotides [13] were purchased from InvivoGen (San Diego, CA, USA) and Sigma Genosys (Ishikari, Japan), respectively. Anti-α-tubulin antibody, Alexa Fluor 594- and 647-conjugated cholera toxin subunit B (CTXb), Alexa Fluor 546-conjugated anti-mouse IgG, Alexa Fluor 594-conjugated phalloidin, rhodamine B-conjugated dextran (MW 10000), and LysoTracker Red DND-99 were purchased from Invitrogen (Carlsbad, CA, USA). Anti-KDEL antibody and anti-58K Golgi protein antibody were purchased from Stressgen (Ann Arbor, MI, USA) and Abcam (Cambridge, UK), respectively. Anti-GFP antibody (clone JL-8) and NF-κB luciferase reporter construct were purchased from Clontech (Mountain View, CA, USA). Anti-HA antibody and anti-FLAG(M2) peroxidase conjugate were purchased from Covance (Berkeley, CA, USA) and Sigma (St. Louis, MO, USA), respectively.

Cells were cultured in Dulbecco's modified Eagle's medium (DMEM) containing 10% fetal bovine serum (FBS). All HEK293T stable transformants were prepared by retroviral gene transfer as described previously [14].

2.2. DNA constructs

The TIR domain-swap mutant (TRIFTIR) was constructed by "PCR sewing" of cDNA corresponding to amino acids 1–160 of mouse MyD88 and amino acids 397–534 of mouse TRIF. The resulting cDNA was cloned into the pMXpie-N-HA retroviral vector. The cDNAs encoding HA-tagged mouse MyD88, HA-tagged TRIFTIR, and FLAG-tagged mouse TIRAP were subcloned into the pMXpie retroviral vector [15] and pEF-BOS-EX vector (a kind gift from Dr. Shigekazu Nagata, Kyoto University [16]). The C-terminal yellow fluorescent protein (YFP)- or cyan fluorescent protein (CFP)-tagged full-length MyD88 (amino acids 1–296), N (amino acids 1–31), N–DD (amino acids 1–109), N–DD–INT (amino acids 1–160), DD–INT–TIR (amino acids 32–296), Δ(1–51) (amino acids 52–296), INT–TIR (amino acids 110–296), TRIFTIR, TLR5, and TLR9 were constructed by subcloning cDNA encoding each protein into pMXrmv5-$(G_4S)_3$YFP or pMXrmv5-$(G_4S)_3$CFP retroviral vectors. YFP or CFP was fused to the C-terminus of the protein of interest via a short linker sequence [(Gly-Gly-Gly-Gly-Ser) × 3] within the vectors. YFP-tagged TLR4 was described previously [17].

2.3. Microscopy

Cell-surface staining with CTXb was performed as described previously [18]. A Z-Stack image was collected using a KEYENCE BZ-9000 fluorescent microscope with step sizes of 0.2 μm.

For the staining of various subcellular markers, cells were fixed and permeabilized with Cytofix/Cytoperm solution (BD Pharmingen, San Diego, CA, USA) and then treated with anti-α-tubulin antibody (1:200 dilution), anti-KDEL antibody (1:200 dilution), or anti-58K Golgi protein antibody (1:250 dilution) for 1 h at 4 °C, followed by Alexa Fluor 546-conjugated anti-mouse IgG antibody (1:200 dilution) for 30 min at 4 °C or Alexa Fluor 594-conjugated phalloidin (1:40 dilution) for 20 min at room temperature. For endosome staining, cells were treated with 1 mg/ml rhodamine B-conjugated dextran for 10 min (early endosome) or 2 h (late endosome) at 37 °C [19]. For lysosome staining, cells were treated with LysoTracker Red DND-99 (1:20000 dilution) for 30 min at 37 °C. The images were acquired using a Bio-Rad MRC1024 laser scanning confocal microscope.

2.4. Gel filtration analysis

HEK293T cells stably expressing MyD88-YFP (HEK293T-MyD88-YFP, 1×10^7) were lysed with 500 μl of lysis buffer (20 mM Tris–HCl, 150 mM NaCl, 2 mM EDTA, 1% Triton X-100, and complete protease inhibitor cocktail [Roche, Mannheim, Germany], pH 7.4). The lysate was centrifuged, and the supernatant was loaded onto a Superose 6 HR10/30 column (GE Healthcare, Little Chalfont, UK). Fractions (0.5 ml) were analyzed by immunoblotting using anti-GFP antibody. The apparent molecular weight was evaluated after column calibration with protein standards: thyroglobulin (669 kDa), ferritin (440 kDa), aldolase (158 kDa), conalbumin (75 kDa), and ovalbumin (43 kDa).

2.5. Luciferase reporter assay

HEK293T cells were plated at a density of 2×10^5 cells/well in a 24-well plate. One day after plating, the cells were transiently transfected with 10 ng of NF-κB luciferase reporter plasmid together with 0.8 μg of retroviral expression plasmid(s). Luciferase activity in the total cell lysate was monitored for 24–48 h after transfection using the dual-luciferase reporter assay system (Promega, Madison, WI, USA).

2.6. Co-imunoprecipitation

Cells (2×10^6) were transiently transfected with 8 μg of pEF-BOS-EX-based expression plasmid(s). Twenty-four hours after transfection, cells were lysed with 600 μl of lysis buffer (50 mM Tris–HCl, 150 mM NaCl, 1% Nonidet P-40, 5 mM EDTA, and protease inhibitor cocktail [Roche], pH 7.5). The supernatants were incubated with anti-GFP antibody for 16 h at 4 °C. Protein G-Sepharose 4 Fast Flow (GE Healthcare) was added and the samples were incubated for 4 h at 4 °C. The beads were washed four times with 1 ml of lysis buffer, boiled with SDS sample buffer, and subjected to immunoblotting using the indicated antibodies.

2.7. GST pull-down assay

GST fusion proteins were expressed in BL21-Gold bacteria by 3 h of induction with 0.1 mM IPTG (isopropyl-β-D(−)-thiogalactopyranoside). Bacterial pellets were resuspended in buffer A, consisting of 5 mM dithiothreitol (DTT) and 1% Triton X-100 in phosphate-buffered saline (PBS; pH 7.4). After sonication, the lysates were centrifuged and the supernatants were incubated with Glutathione-Sepharose 4B (GE Healthcare) for 1 h at 4 °C. The beads were washed five times with 1 ml of buffer A and resuspended in lysis buffer to prepare a 50% slurry.

HEK293TCM cells [17] stably expressing TLR4-YFP (HEK293TCM-TLR4-YFP; 6×10^6) were transfected with 24 μg of empty vector or pEF-BOS-EX-TIRAP-FLAG. After 48 h, lysates were prepared, and the supernatants were incubated with 10 μg of GST fusion proteins for 1 h at 4 °C. The GST fusion protein-bound beads were washed three times with lysis buffer, boiled with SDS sample buffer, and subjected to immunoblotting using anti-FLAG antibody.

3. Results and discussion

3.1. MyD88 is localized in the cytoplasm in condensed, morphologically diverse forms

Previous studies have shown that MyD88 is present in discrete foci scattered throughout the cytosol [9–11]. We also observed this distinct characteristic using MyD88-YFP fusion proteins in HEK293T cells (Fig. 1A) and bone marrow-derived macrophages (data not shown). MyD88-YFP induced NF-κB activation when over-expressed (Fig. 1B) and mediated TLR signaling in a ligand-dependent manner (Fig. 5A), indicating that the MyD88-YFP fusion protein is functional. The Z-Stack image collected from wide-field microscopy showed that the MyD88-YFP signals were morphologically diverse (Fig. 1C), belonging to one of five typical morphologies: spot, star, string, ring, and cocoon (Fig. 1D). The over-expressed proteins are sometimes misfolded and form aggregates in the cytoplasm, causing improper subcellular distribution. To rule out the possibility that this distinct subcellular localization of MyD88-YFP was an artifact of over-expression, we performed gel filtration analysis to fractionate lysates from HEK293T-MyD88-YFP cells based on molecular size. MyD88-YFP, which has a calculated molecular size of 61.8 kDa, was detected in fractions numbers. 32 and 33, corresponding to 67 kDa and 132 kDa, respectively (Fig. 1E). These data indicate that MyD88-YFP is present as a monomer and/or homodimer in the cytoplasm, which is consistent with earlier observations by Burns et al. [5], who found that MyD88 forms

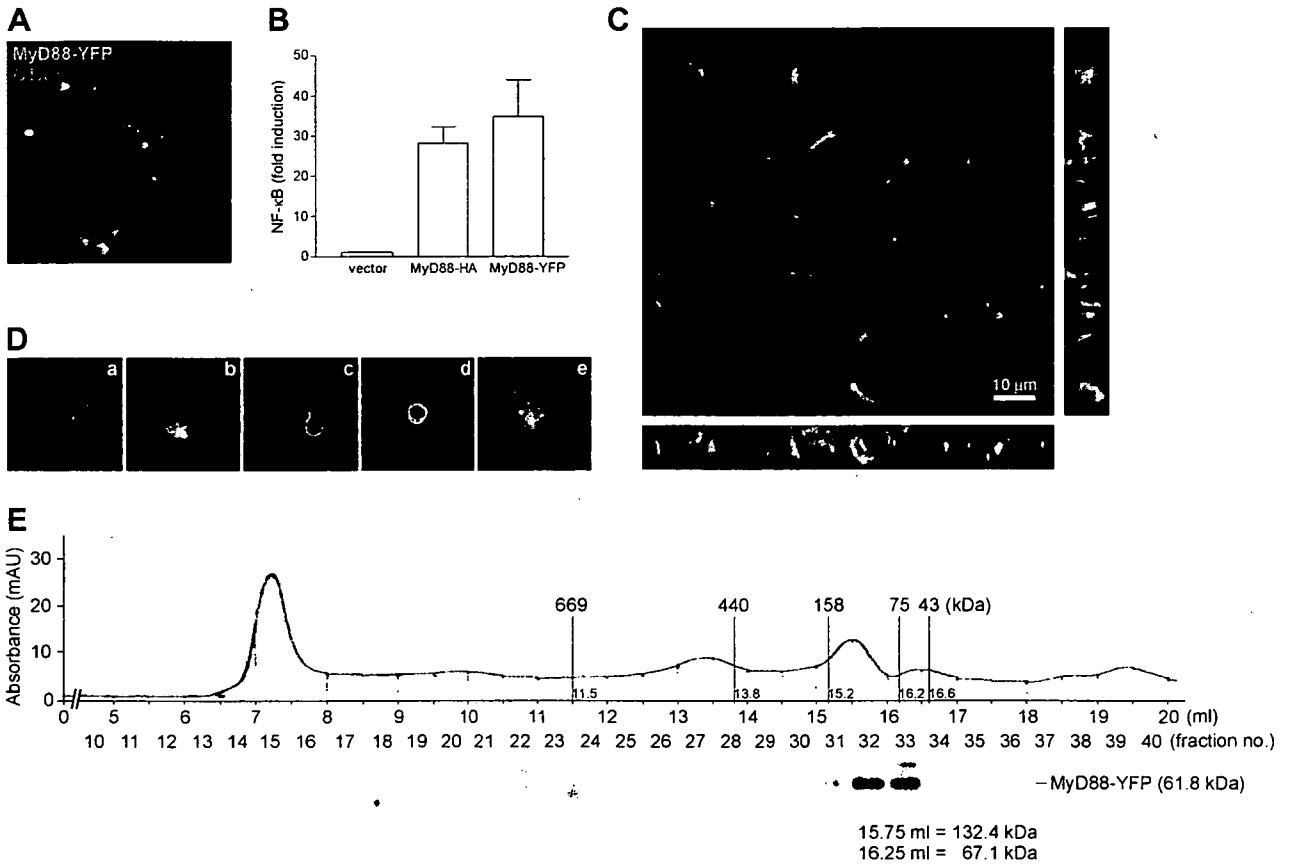

Fig. 1. MyD88 is localized in the cytoplasm as large condensed forms. (A) Confocal image of HEK293T-MyD88-YFP cells stained with Alexa Fluor 594-conjugated CTXb. (B) HEK293T cells were transiently transfected with 0.8 μg of the indicated expression plasmids along with 10 ng of NF-κB reporter construct. Luciferase activity was measured 24 h after transfection. Results are shown as the means ± standard deviation of three independent experiments. (C) Z-Stack image of MyD88-YFP in HEK293T cells. (D) Typical morphologies of MyD88-YFP in HEK293T cells: (a) spot; (b) star; (c) string; (d), ring; (e), cocoon. (E) HEK293T-MyD88-YFP cells were lysed and fractionated on a Superose 6 gel filtration column. MyD88-YFP was analyzed by immunoblotting using anti-GFP antibody. The elution positions of molecular weight markers (in kDa) and the protein concentration of the eluent monitored in real-time (mAU) are indicated.

a homodimer. Therefore, we concluded that the unusual subcellular localization of MyD88-YFP is not an artifact, but instead a characteristic of endogenous MyD88.

3.2. MyD88 localizes to specific intracellular organelles

Our data from microscopy and gel filtration analysis suggest that MyD88 is present in vesicle-like structures or associated with tubular or fibrillar structures. To identify the intracellular compartments in which MyD88 is enriched, HEK293T-MyD88-YFP cells were stained with markers for the endoplasmic reticulum (ER), Golgi apparatus, endosomes, and lysosomes. This experiment was based on observations that some of the morphologies of MyD88-YFP are similar to the morphologies of these organelles; in addition, TLRs have been identified in these compartments [20–23]. We used the following markers: proteins containing a C-terminal KDEL sequence for the ER, 58K Golgi proteins for the Golgi apparatus, dextran for early and late endosomes, and LysoTracker for lysosomes. However, no clear co-localization of MyD88-YFP and these markers was observed (Fig. 2). We also examined the co-localization of MyD88 with cytoskeletal proteins such as F-actin and α-tubulin. This was based on observations that some of the morphologies of MyD88-YFP appeared similar to those of the cytoskeletal structures; furthermore, MyD88 is associated with fibrillar aggregates containing β-actin in the cytoplasm [8]. However, neither F-actin (phalloidin staining) nor α-tubulin was clearly co-localized with MyD88-YFP (Fig. 2). These results suggest that MyD88 resides in as yet uncharacterized organelles.

3.3. The entire non-TIR region is required for the distinct subcellular localization of MyD88

Typical sequences for targeting proteins to intracellular compartments, such as the KDEL sequence in ER proteins, have not been identified in MyD88. The primary structure of MyD88 can be divided into four regions: the N-terminal short region (N), a death domain (DD), an intermediate region (INT), and a TIR domain [5]. Therefore, we investigated which regions are involved in the subcellular localization of MyD88. We generated several truncated mutants of MyD88 and a TIR domain-swap mutant (TRIFTIR) in which the TIR domain of MyD88 was replaced with the corresponding region of TRIF [24,25] (Fig. 3A). The mutant proteins fused with YFP at the C-terminus were expressed in HEK293T cells, and the subcellular localization was examined under a microscope. The TRIFTIR mutant and the TIR domain-deleted mutant (N-DD-INT) were localized in the cytoplasm in condensed form (Fig. 3B). Furthermore, these mutants were clearly co-local-

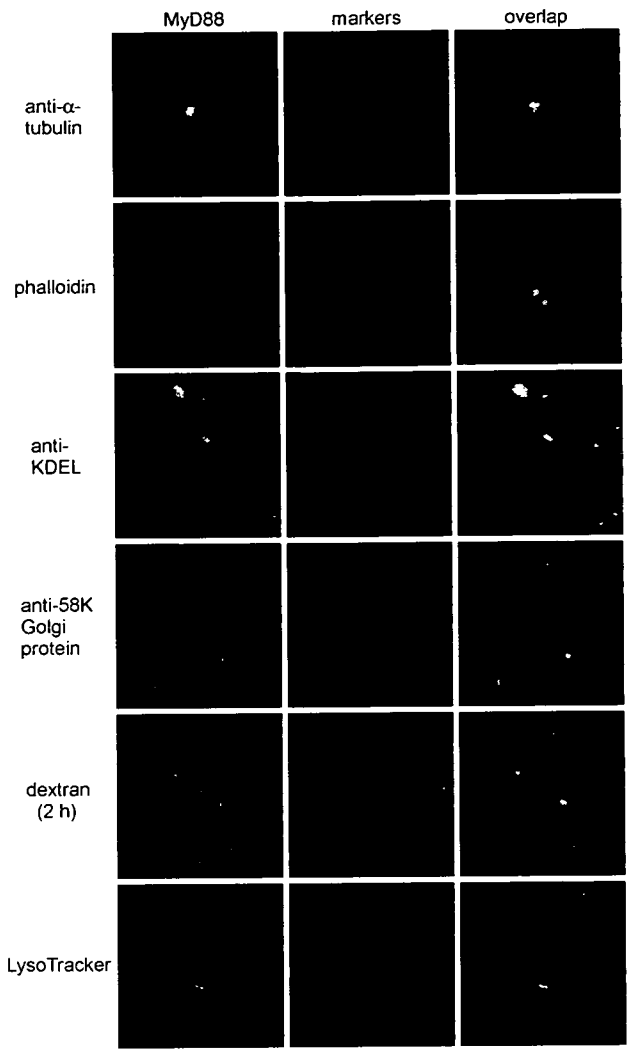

Fig. 2. MyD88 resides in uncharacterized organelles in HEK293T cells. HEK293T-MyD88-YFP cells were stained with the indicated markers as described in Section 2. For LysoTracker staining, the cells were counterstained with CTXb to visualize the cell surface [blue (pseudocolor)].

ized with wild-type MyD88 in the cytoplasm (Fig. 3C and D). In contrast, all other mutants lacking a part of the non-TIR region were diffusely expressed throughout the cytoplasm and/or nucleus. These results suggest that the entire non-TIR region plays a critical role in localizing MyD88 within the cell.

3.4. Correct cellular targeting of MyD88 is critical to the activation of signaling events

The functional significance of this distinct subcellular localization is unclear. MyD88 associates with downstream signaling molecules such as interleukin-1 receptor-associated kinase 1 (IRAK1) [3] and IRF-7 [12] through its DD. Therefore, we used DD-containing MyD88 mutants to examine the significance of the subcellular localization in signal transduction. MyD88 and its mutants were over-expressed in HEK293T cells, and NF-κB activity was measured using a reporter assay. Interestingly, the TRIFTIR and N–DD–INT mutants that were co-localized with wild-type MyD88 induced NF-κB activation, whereas the N-DD and DD–INT–TIR mutants

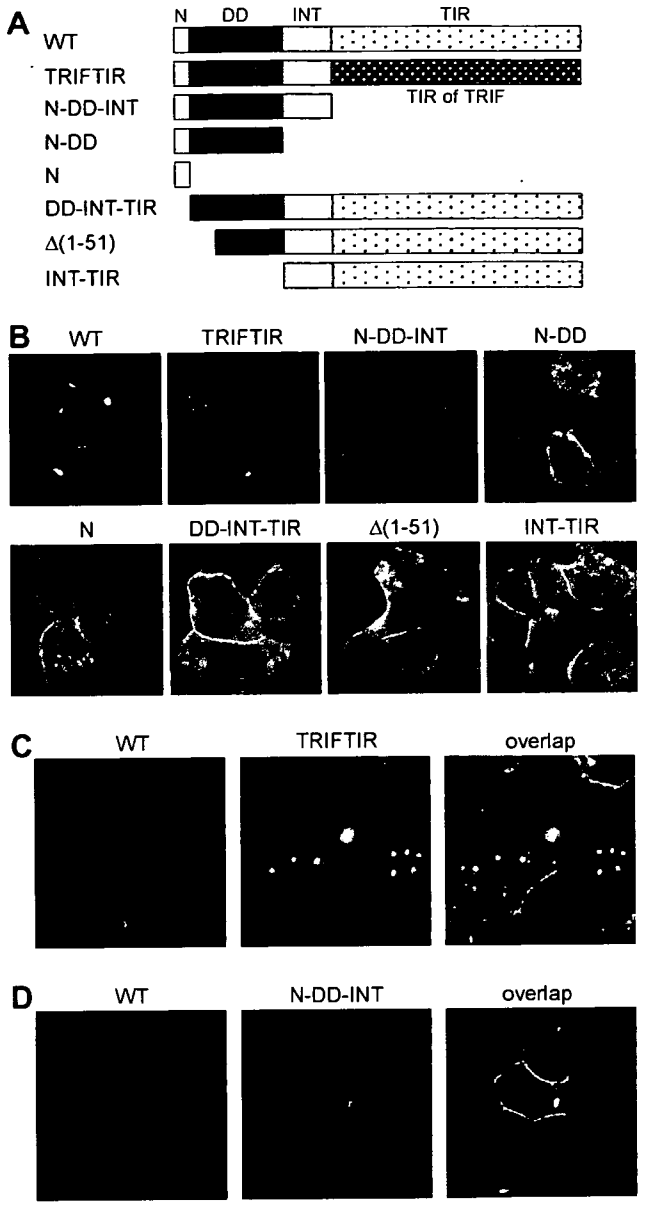

Fig. 3. The entire non-TIR region is responsible for the distinct subcellular localization of MyD88. (A) Schematic diagram of MyD88 mutant proteins. (B) Confocal images of HEK293T cells expressing the proteins depicted in A. The images were created as described in Fig. 1A. MyD88 and its mutant proteins are shown in green; CTXb is shown in red. (C, D) Confocal images of HEK293T cells expressing MyD88-CFP and TRIFTIR-YFP (C) or N–DD–INT–YFP (D). The images were created as described in Fig. 1A. MyD88-CFP is shown in red (pseudocolor); TRIFTIR-YFP and N–DD–INT–YFP are shown in green; CTXb is shown is light blue (pseudocolor); co-localized signals appear yellow.

that were diffusely expressed throughout the cytoplasm and nucleus did not (Fig. 4). These results suggest that the correct cellular localization is essential for the activation of signaling events.

3.5. The specificity of TLR-MyD88 interaction is determined by the conformational characteristics of the TIR domain

Each TLR interacts with specific TIR adaptors, allowing the innate immune system to induce distinct physiological

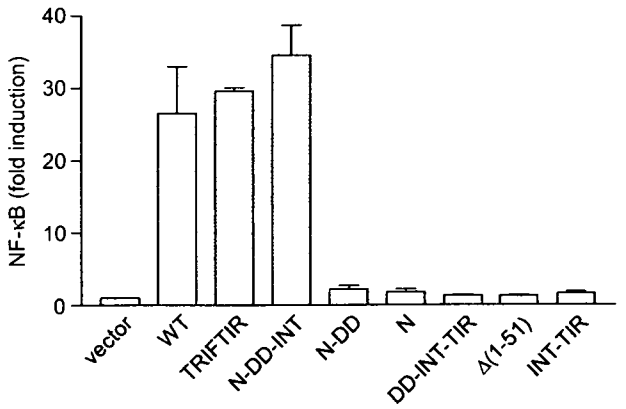

Fig. 4. Correlation between subcellular localization of MyD88 and its signaling function. HEK293T cells were transfected with 0.8 μg of expression plasmids encoding the proteins depicted in Fig. 3A along with 10 ng of NF-κB reporter construct. Luciferase activity was measured 24 h after transfection. Results are shown as the means ± standard deviation of three independent experiments.

responses to distinct infectious microorganisms [26]. There are two factors that may determine the specificity of the TLR–TIR adaptor interaction: the conformational characteristics of each TIR domain (i.e., a mechanical factor) and the distinct subcellular localizations of TLRs and TIR adaptors (i.e., a spatiotemporal factor). Both TLR5 and TLR9 signaling are totally dependent on MyD88, but not other TIR adaptors [2]. To identify the mechanism that determines the interaction specificity between these proteins, wild-type MyD88 and the TRIFTIR mutant were co-expressed with TLR5 or TLR9 in HEK293T cells. The cells were stimulated with flagellin for TLR5 or CpG-B for TLR9, and NF-κB activity was measured using a reporter assay. Ligand-dependent NF-κB activation was observed in the cells expressing MyD88, but not in those expressing the TRIFTIR mutant, although wild-type MyD88 and the TRIFTIR mutant show similar constitutive activities (Fig. 5A). Given that the TRIFTIR mutant co-localizes with wild-type MyD88, these results suggest that the specificity of the interaction between MyD88 and TLR5 or TLR9 is determined by the conformational characteristics of each TIR domain; the TIR domain of MyD88 has a high affinity for TLR5/9, whereas the TIR domain of TRIF has low affinity.

We performed co-immunoprecipitation analysis to examine the physical interaction between TLR and MyD88. Consistent with the results from the NF-κB reporter assay, MyD88 co-immunoprecipitated with TLR5 in a ligand-dependent manner, whereas the TRIFTIR mutant did not co-immunoprecipitate (Fig. 5B). These results demonstrate that the specificity of the TLR–MyD88 interaction is determined by the conformational characteristics of each TIR domain, rather than the spatiotemporal characteristics of the subcellular localization of TLRs and MyD88.

3.6. *The specificity of the MyD88–TIRAP interaction is independent of the conformational characteristics of the TIR domain*

The association of MyD88 with TLR4 is distinct from its association with TLR5 or TLR9. TLR4 requires another TIR adaptor, TIRAP, to associate with MyD88 and activate the MyD88-dependent signaling pathway [27,28]. TIRAP specifically associates with MyD88 via TIR–TIR interaction and facilitates the delivery of MyD88 to activated TLR4 [11]. Because TIRAP forms a heterodimer with MyD88 [27,28], we expected that the specificity of the MyD88–TIRAP interaction is also determined by the conformational characteristics of each TIR domain. To test this assumption, the effect of wild-type MyD88 and the TRIFTIR mutant on TLR4-induced NF-κB activation was examined. HEK293T cells stably expressing CD14 and MD-2 (HEK293TCM cells [17]) were transiently transfected with TLR4 and wild-type MyD88 or TRIFTIR mutant, and then NF-κB activity was measured using a reporter assay. Surprisingly, TLR4 and the TRIFTIR mutant synergistically induced NF-κB activation; the activity in cells co-expressing both TLR4 and the TRIF-TIR mutant was much higher (21.7 ± 2.2-fold increase) than the activity estimated by summing the values from cells expressing TLR4 alone and cells expressing TRIFTIR alone

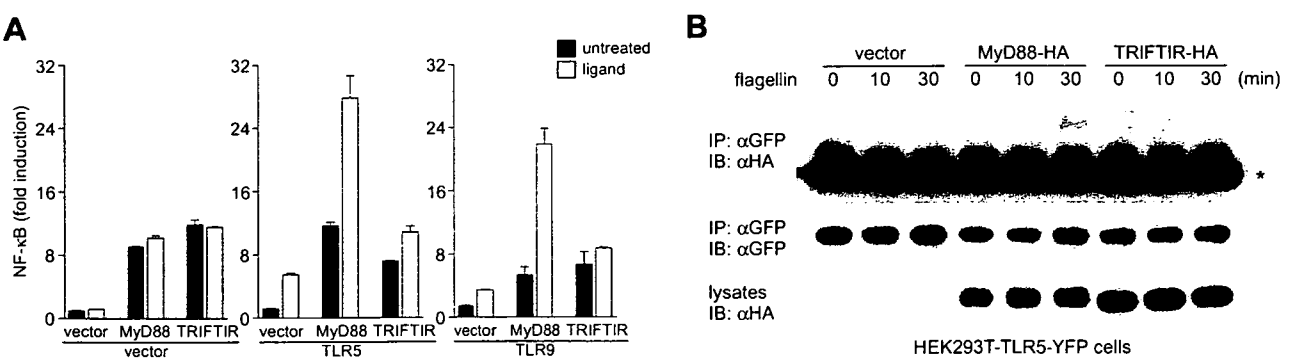

Fig. 5. The interaction of MyD88 with specific TLRs is dependent on the conformational characteristics of the TIR domain. (A) HEK293T cells were co-transfected with 10 ng of NF-κB reporter construct and the expression plasmids for the indicated combinations of empty vector (0.1 or 0.7 μg), MyD88 (0.1 μg), TRIFTIR (0.1 μg), TLR5-YFP (0.7 μg), and TLR9-YFP (0.7 μg). After 24 h, the cells were treated with 100 ng/ml flagellin for vector and TLR5 or 5 μM CpG-B for TLR9 and further incubated for 16 h at 37 °C. NF-κB-dependent luciferase activity was then analyzed. Results are shown as the means ± standard deviation of three independent experiments. (B) HEK293T cells stably expressing TLR5-YFP (HEK293T-TLR5-YFP) were transfected with empty vector, MyD88-HA, or TRIFTIR-HA. After 24 h, the cells were stimulated with 100 ng/ml flagellin at the indicated times. Lysates were prepared, and co-immunoprecipitation analysis was performed as described in Section 2. Lysates were analyzed to confirm the equivalent expression of the appropriate proteins in each sample. The asterisk next to the upper panel shows the immunoglobulin light chain of anti-GFP antibody used in the immunoprecipitation.